



University of  
**Strathclyde**  
Glasgow

Ion acceleration as a diagnostic of  
fast electron transport in solid targets  
(+ nuclear activation as an ion beam diagnostic)

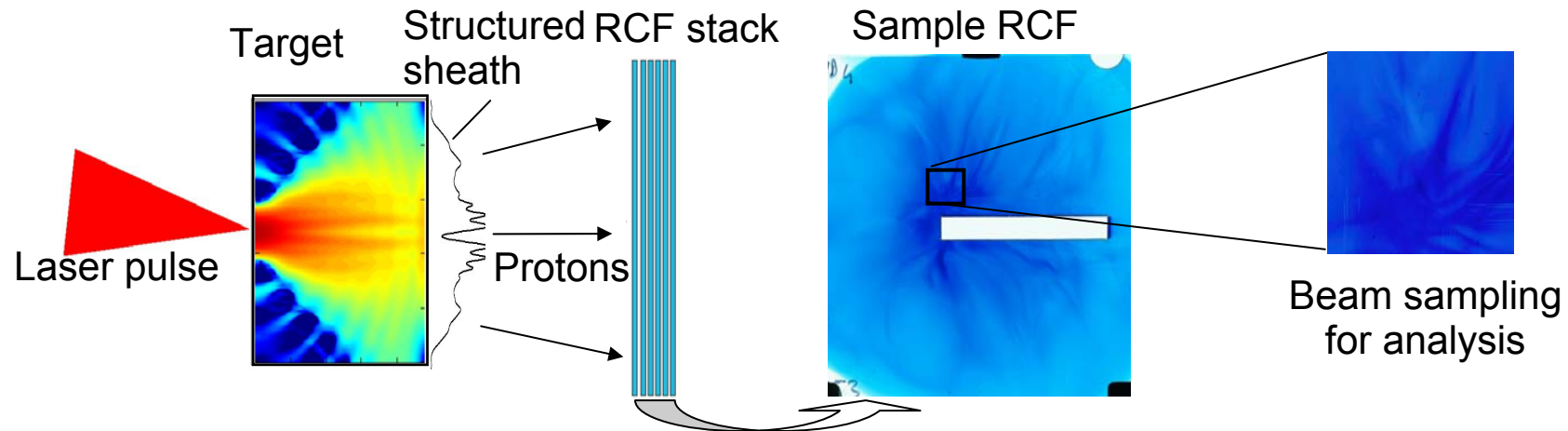
Paul McKenna

University of Strathclyde



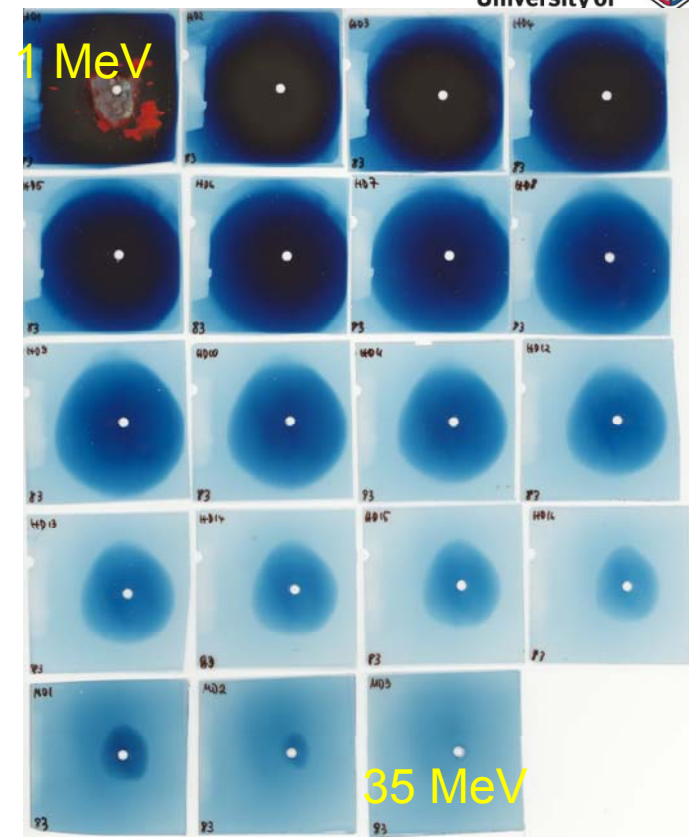
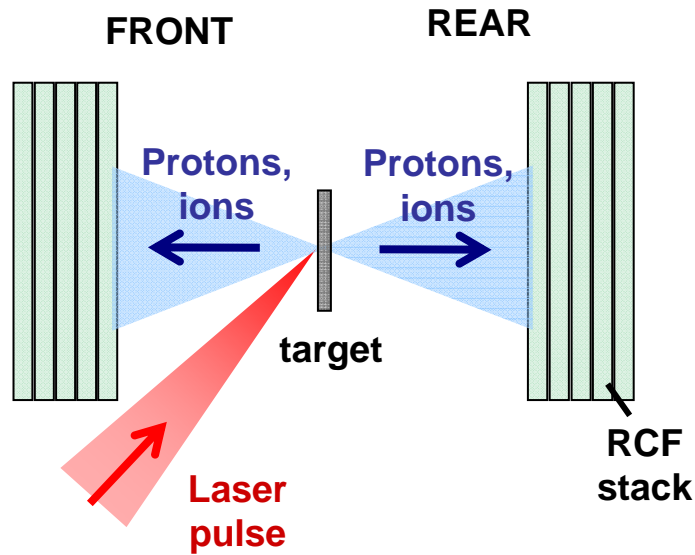


## Proton emission as a diagnostic



- Maximum proton energy → electron density
- Intensity distribution → electron transport filamentation
- Proton divergence with energy → electron sheath profile
- Total ion energy → laser to electron energy transfer
- Proton spectrum → electron temperature (model)

# Dosimetry film stack diagnostic



Three main types of dosimetry film:

## MD-55

Clear Polyester - 67 microns
Active layer - 16 microns
Adhesive - 25 microns
Clear Polyester - 25 microns
Adhesive - 25 microns
Active layer - 16 microns
Clear Polyester - 67 microns

## HD-810

Surface layer - 0.75 microns
Active layer - 6.5 microns
Clear Polyester - 97 microns

## HS

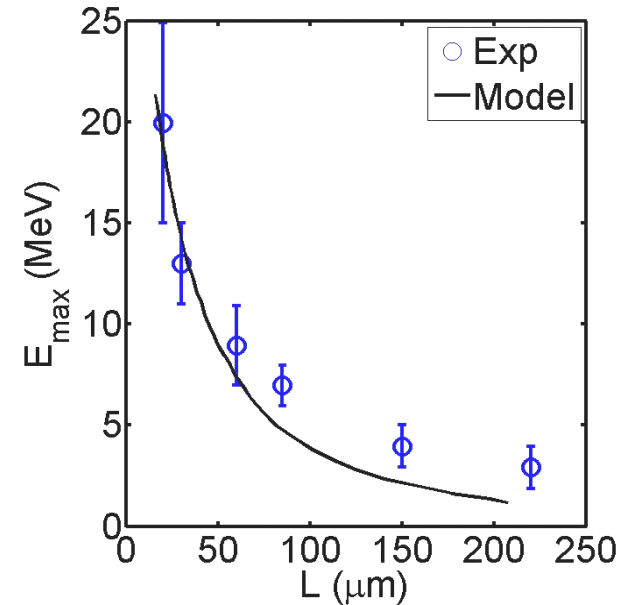
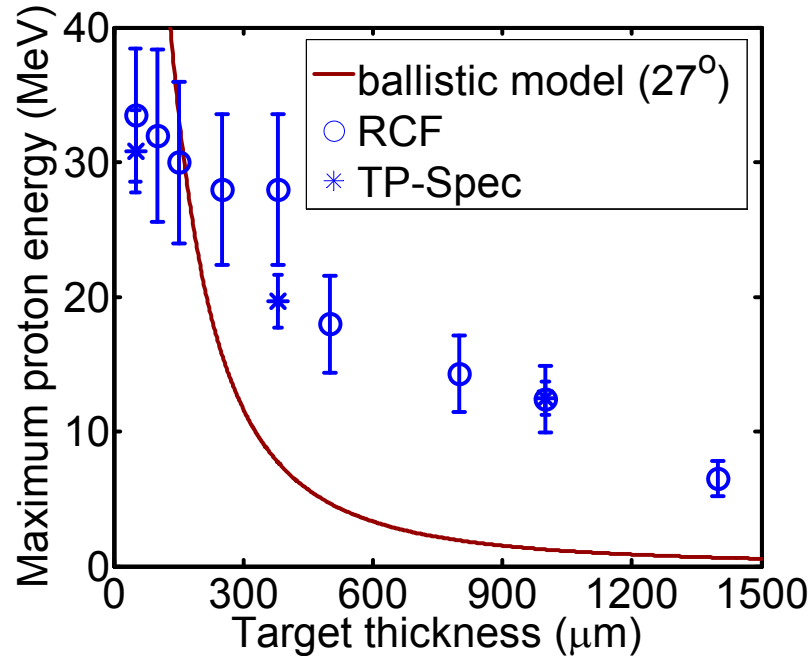
Clear Polyester - 97 microns
Active layer - 40 microns
Clear Polyester - 97 microns



# 1. Proton energy as a diagnostic of fast electron beam divergence



## Results: Maximum proton energy



Fuchs et al., LULI (Nat. Phys. 2006)

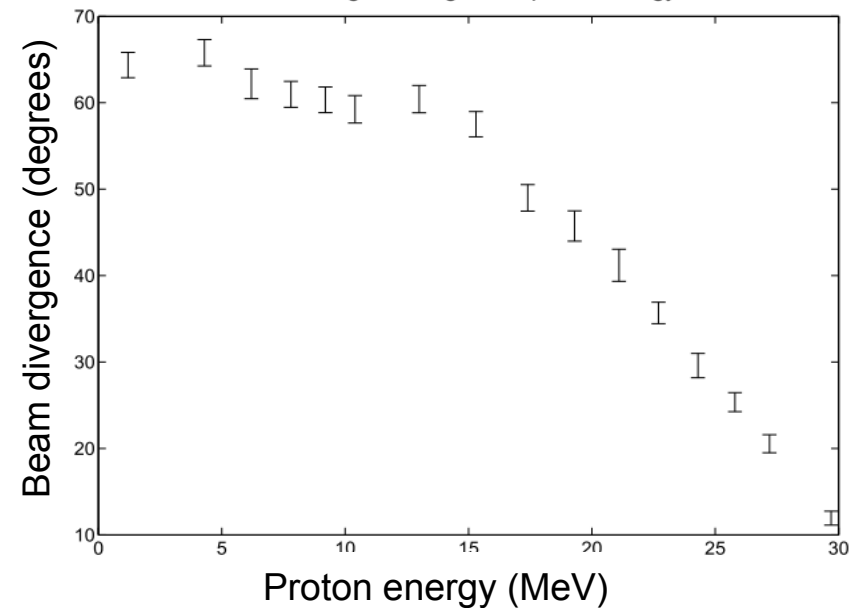
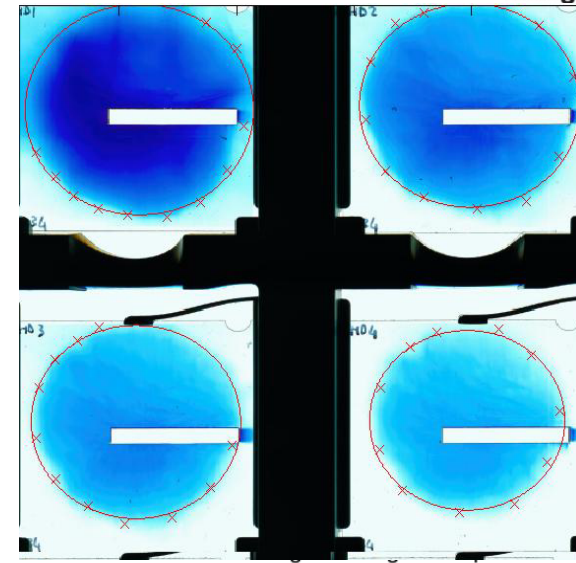
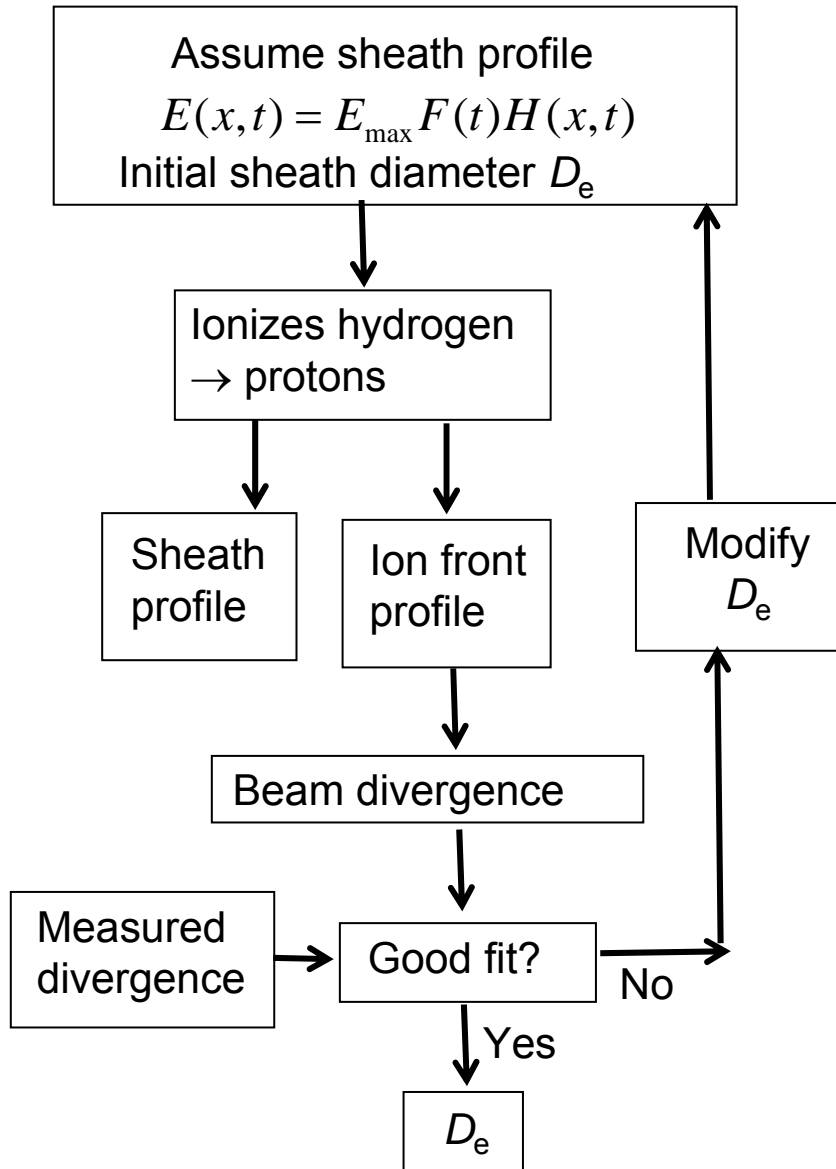
Ballistic transport and P. Mora PRL 2003 plasma expansion model.

$$E_p \approx 2k_B T [\ln(\tau + \sqrt{\tau^2 + 1})]^2, \quad \tau = t_i \omega_{pp} / \sqrt{2e_N}, \quad \omega_{pp} \sim \sqrt{n_e} \sim 1 / \phi_{sheath}$$

The scaling with target thickness is significantly different than expected from ballistic electron transport

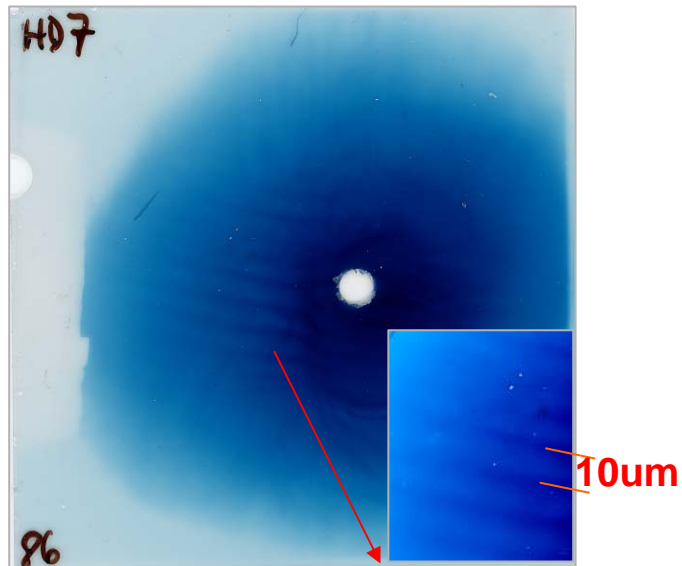
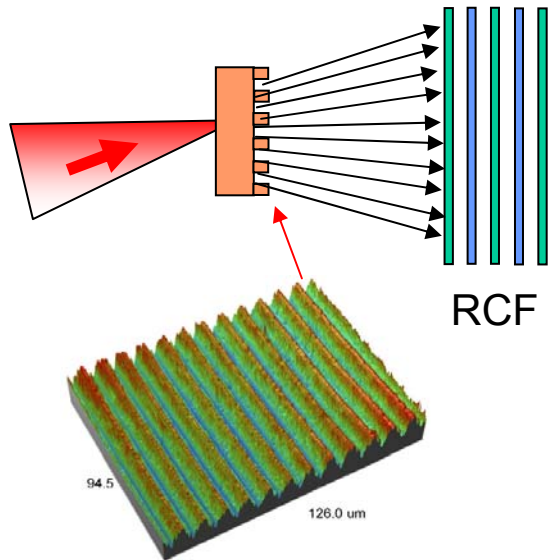


# Sheath expansion is modelled

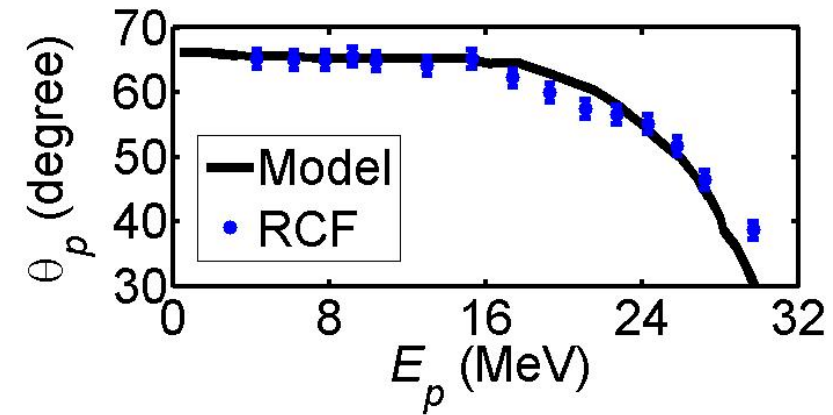




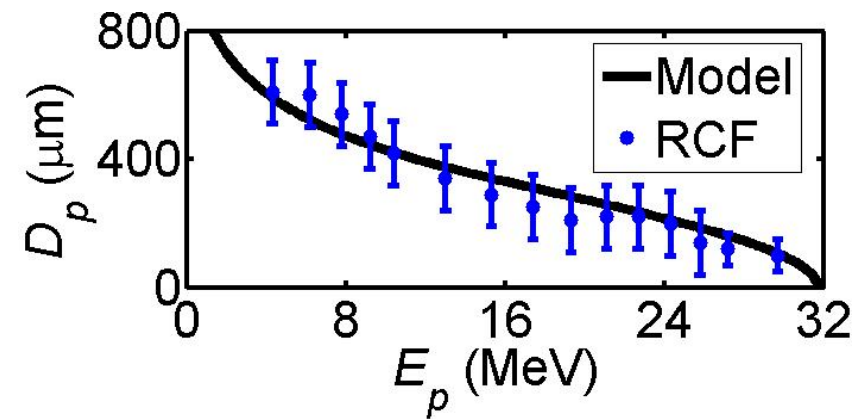
# Model is benchmarked using 'grooved' target results



### Divergence

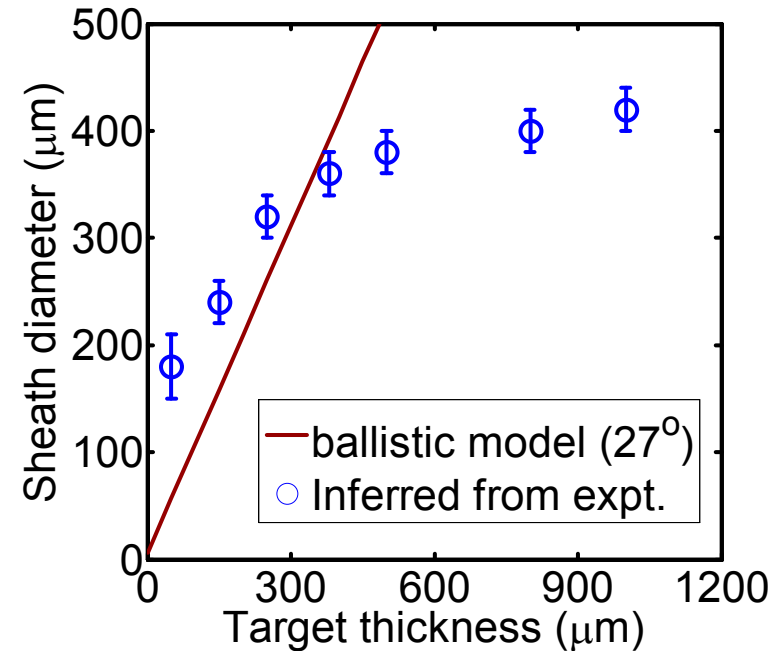
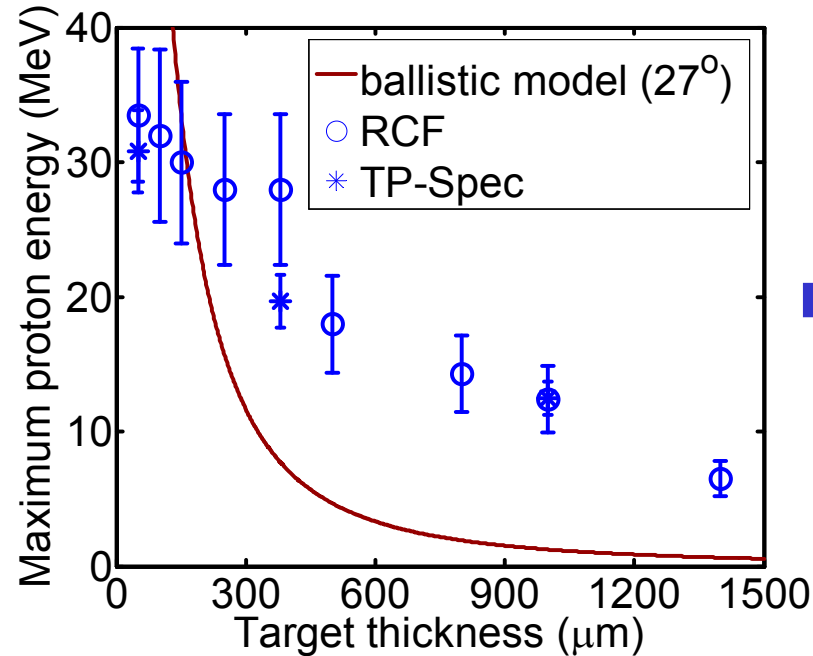


### Source size





# Proton emission as a function of target thickness

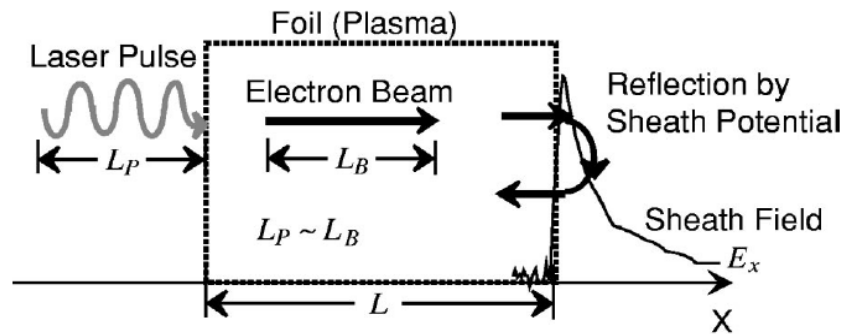


- Evidence of a restriction in lateral spreading of fast electrons within the target
- Self-generated B-field is an obvious candidate
- But why should this depend on the target thickness?

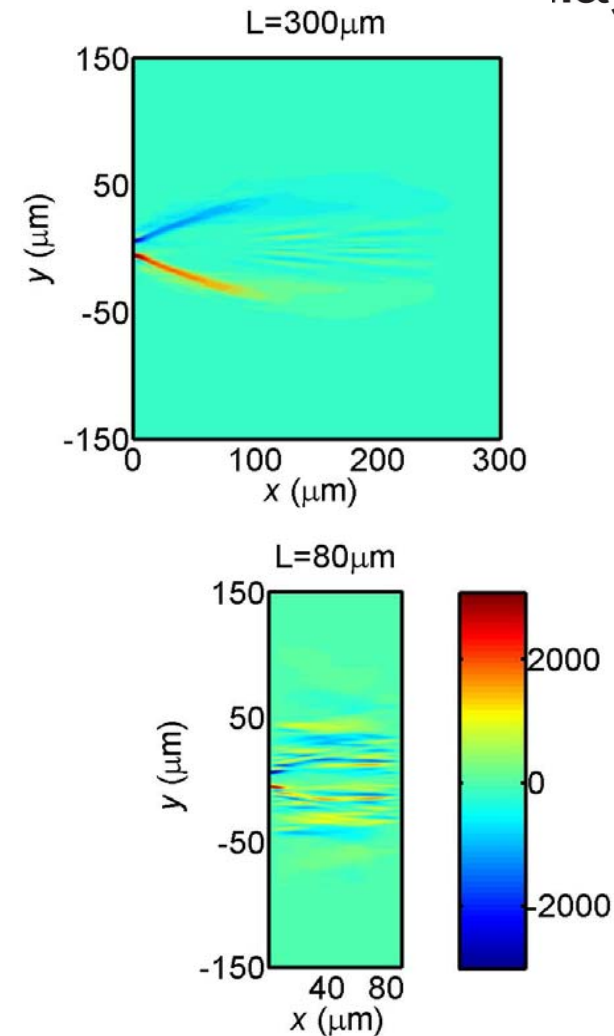
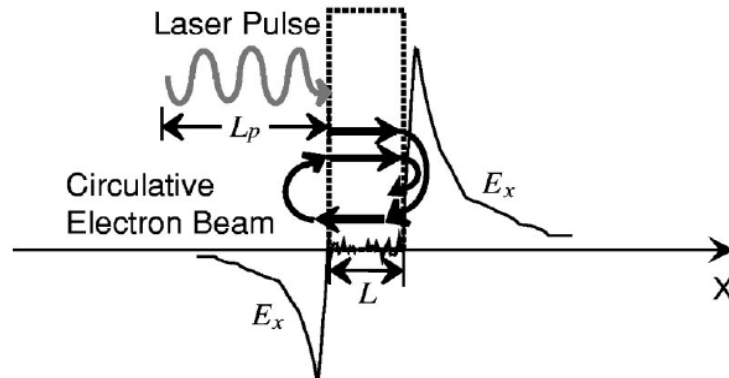


# Fast electron refluxing

(I)  $L > L_p/2$



(II)  $L < L_p/2$



Sentoku *et al*, Phys Plasmas, 10, 2009 (2003) Electron refluxing within thin targets perturbs B-field and therefore collimation

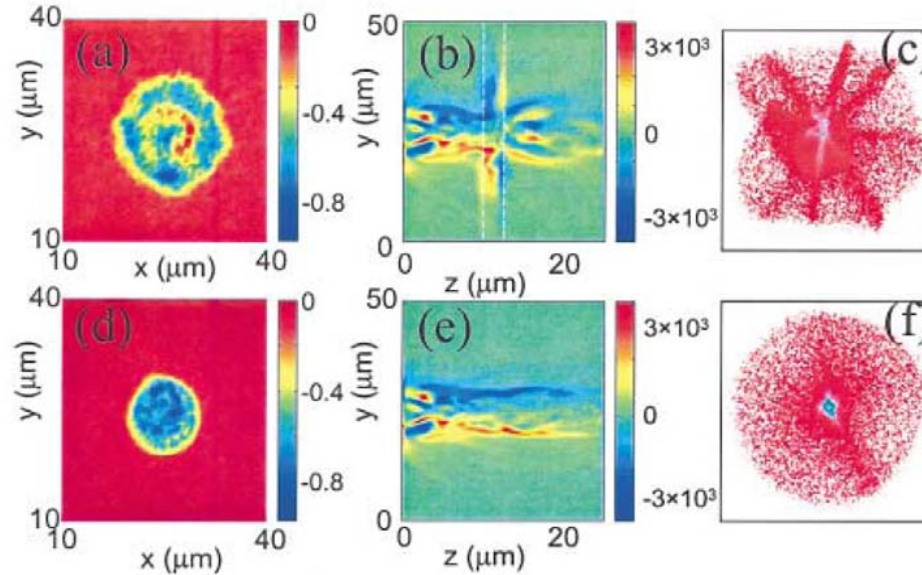
X. H. Yuan *et al*, New Journal of Physics 12 063018 (2010)



## 2. Proton spatial-intensity distribution as a diagnostic of fast electron beam filamentation

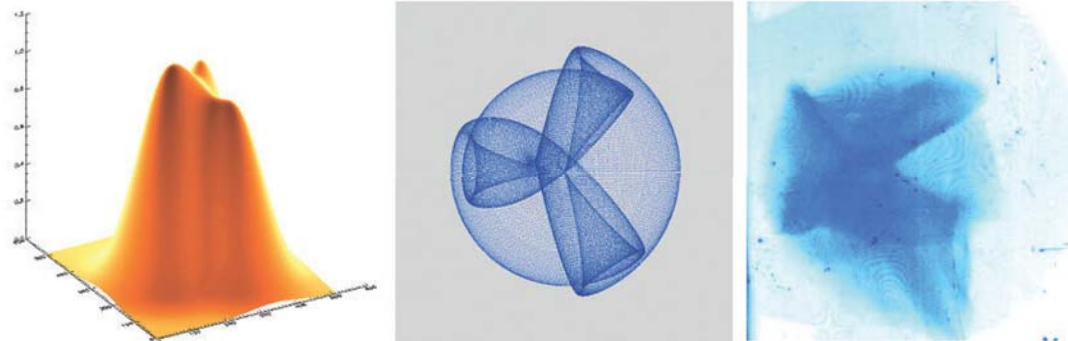
# Mapping of electron distribution into protons

Simulated electron density → Simulated Proton Beam



J Fuchs et al. Phys. Rev. Lett. 91, 255002 (2003).

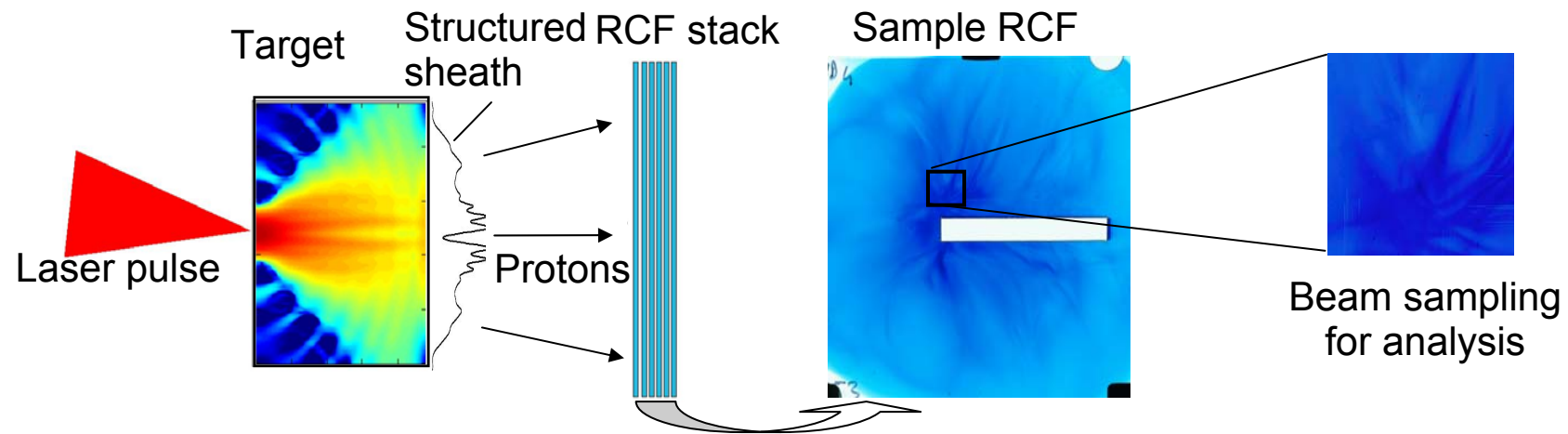
Simulated electron sheath → Simulated Proton Beam → RCF



M Roth, M. et al. PPCF 44, B99 (2002).



# Effects of target material on beam filamentation



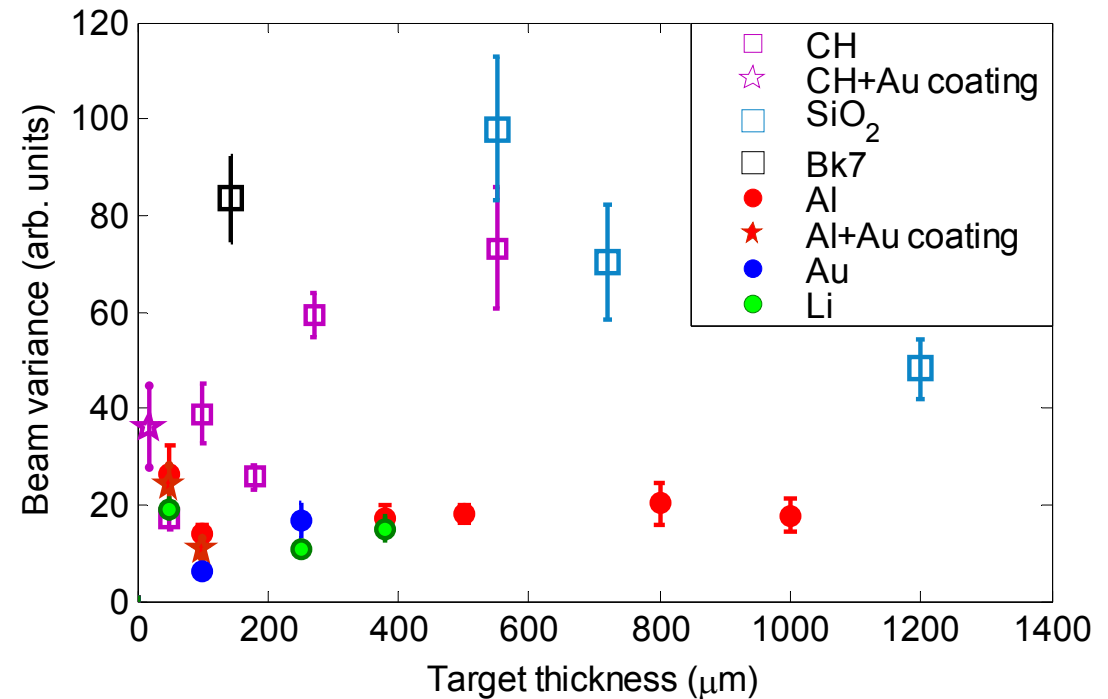
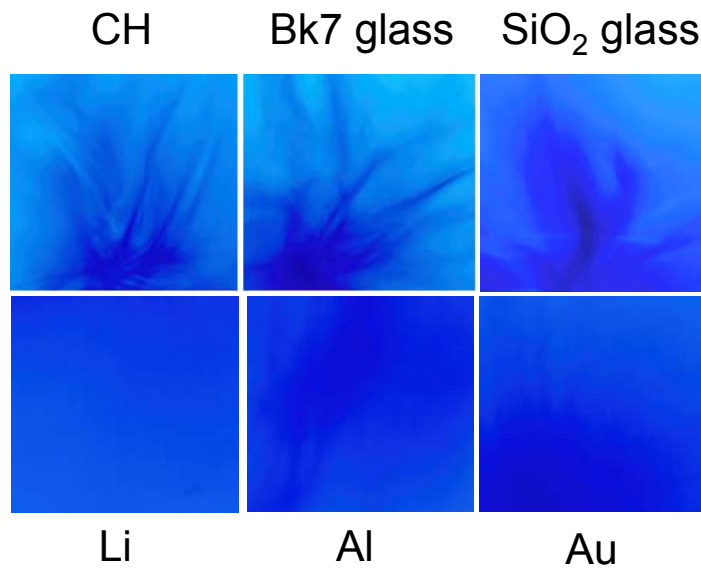
Differences in electron transport in CH & Al target – why?

- Resistive effects?
- Scattering/transverse temperature?

Target	Effective Z	Resistivity [ $\Omega.m$ ]
Al	13	$10^{-8}$
CH	3	$10^{13}$
Li	3	$10^{-7}$
SiO <sub>2</sub>	12	$10^{14}$



# Effects of target material on beam filamentation



Filamentation is independent of target Z and therefore beam transverse temperature (for PW parameters)

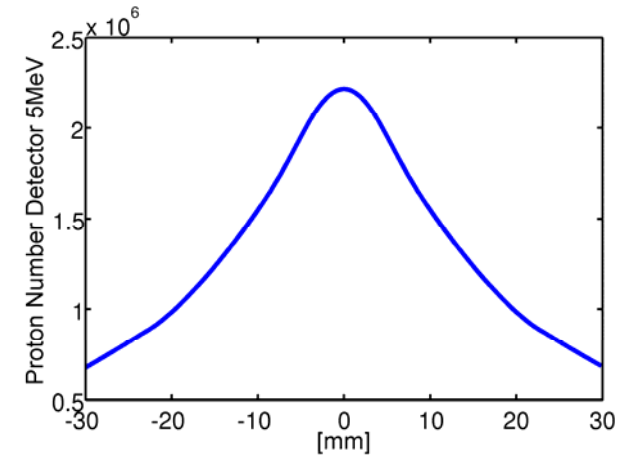
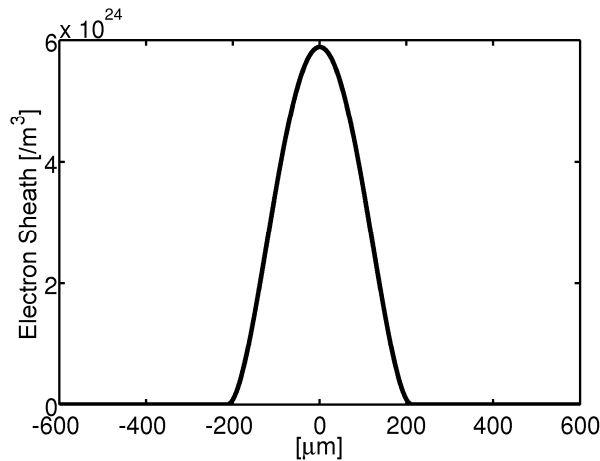


# Analytical model of sheath profile mapping under development (Mark Quinn)

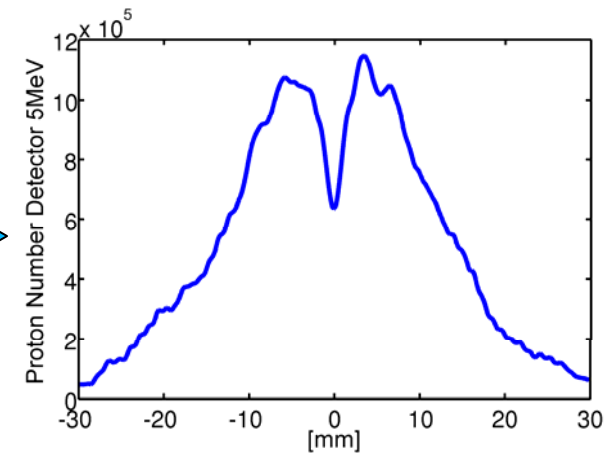
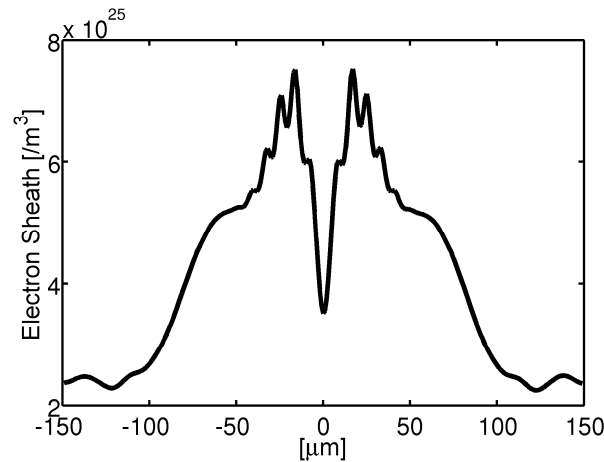
Electron density profile in sheath from hybrid transport simulation

Predicted proton distribution at detector plane (5 MeV)

**Al**



**CH**

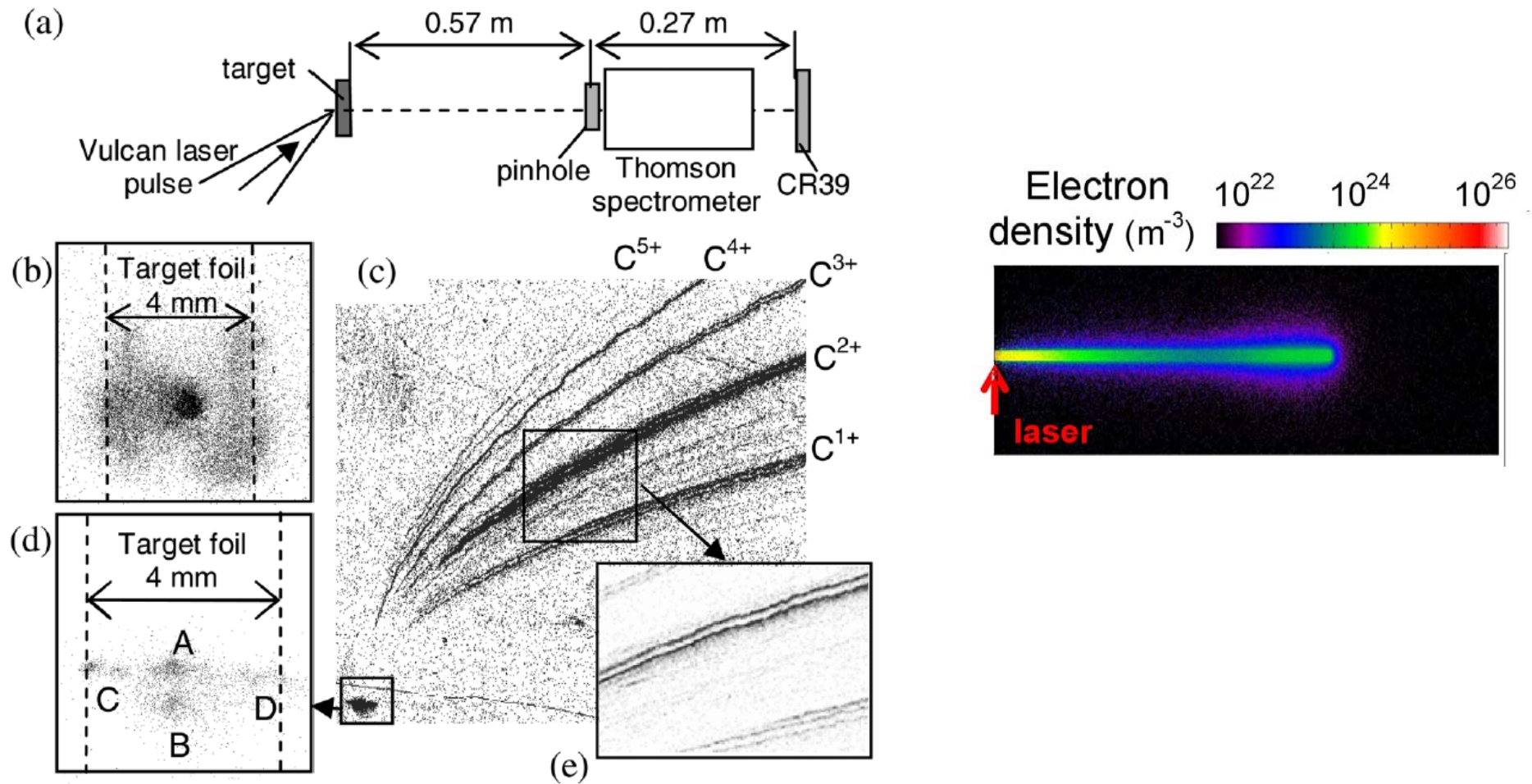




### 3. Ion pinhole imaging as a diagnostic of lateral transport of fast electrons



# Lateral fast electron transport in thin foils



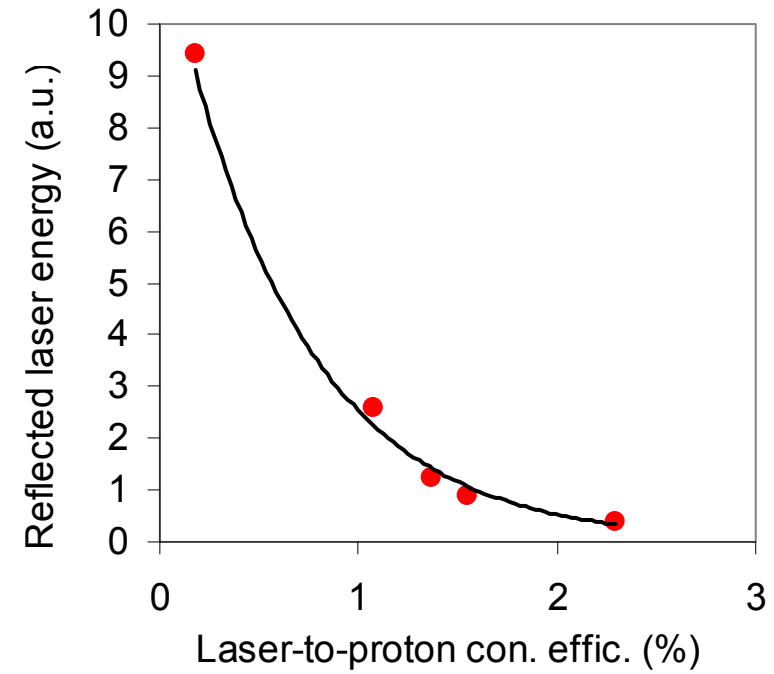
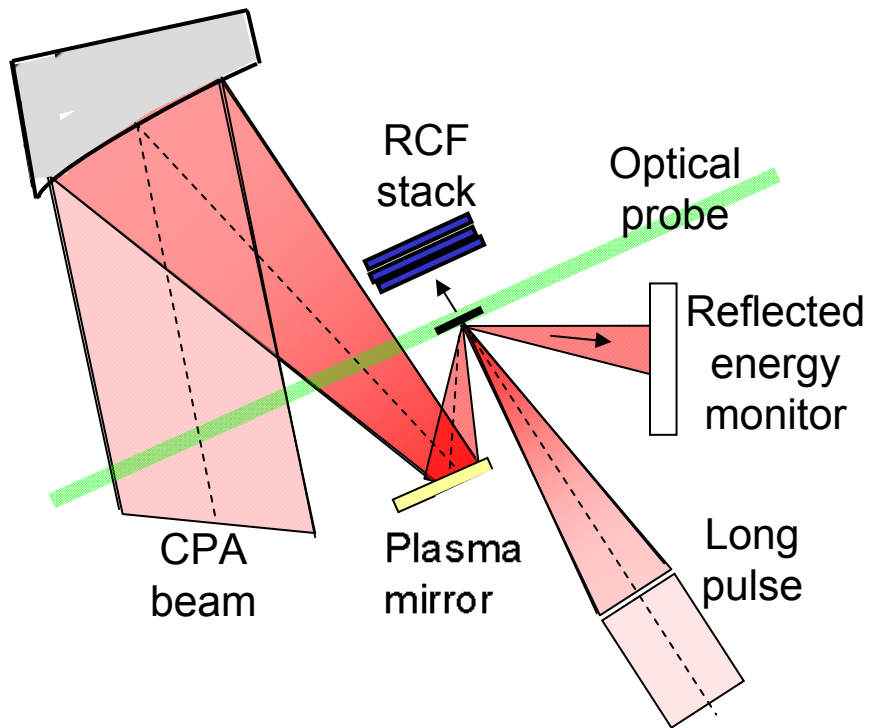




## 4. Total proton energy as a diagnostic of laser-to-electron energy transfer

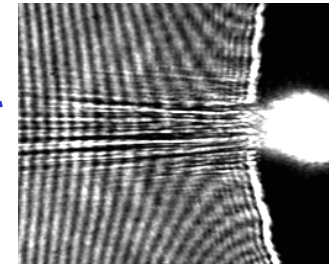
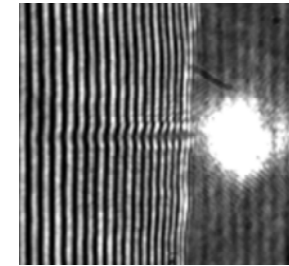
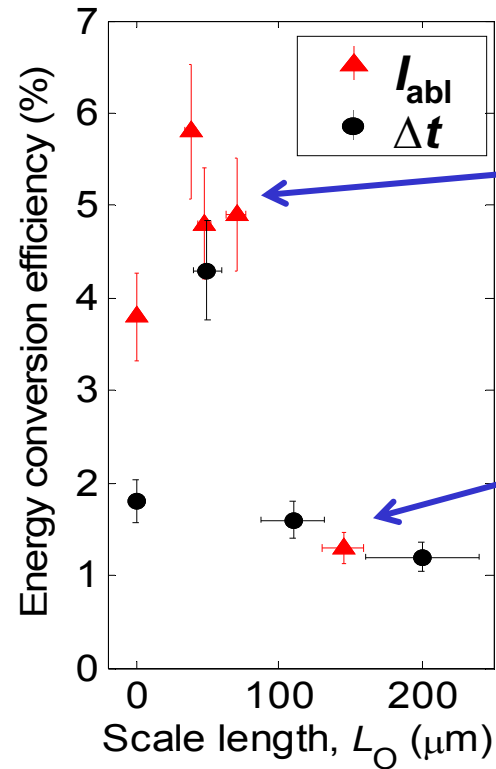
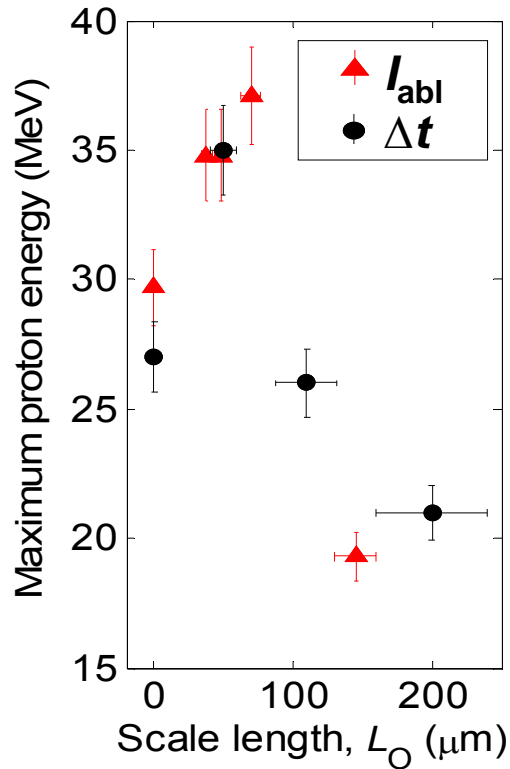


# Total proton energy as a diagnostic of absorption





## Example results



→ Proton measurements show that controlled preplasma expansion leads to enhanced energy coupling to fast electrons

P. McKenna et al, LPB **26** 591-596 (2008)

D.C. Carroll et al, CRP **10** 188-196 (2009)



## 5. Nuclear activation as a diagnostic of proton and ion acceleration



## Nuclear activation as a diagnostic

Diagnostic of particles and radiation above a few MeV

Number of reactions:

$$N = D \int_{E_{Thres.}}^{\infty} \sigma(E) I(E) l(E) dE$$

$D$  Number density of sample

$\sigma(E)$  Cross section

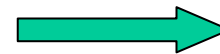
$I(E)$  Photon/Particle distribution

$l(E)$  Stopping range (Sample thickness)

Single activation foil: measure at least 2 reactions with different cross sections

OR

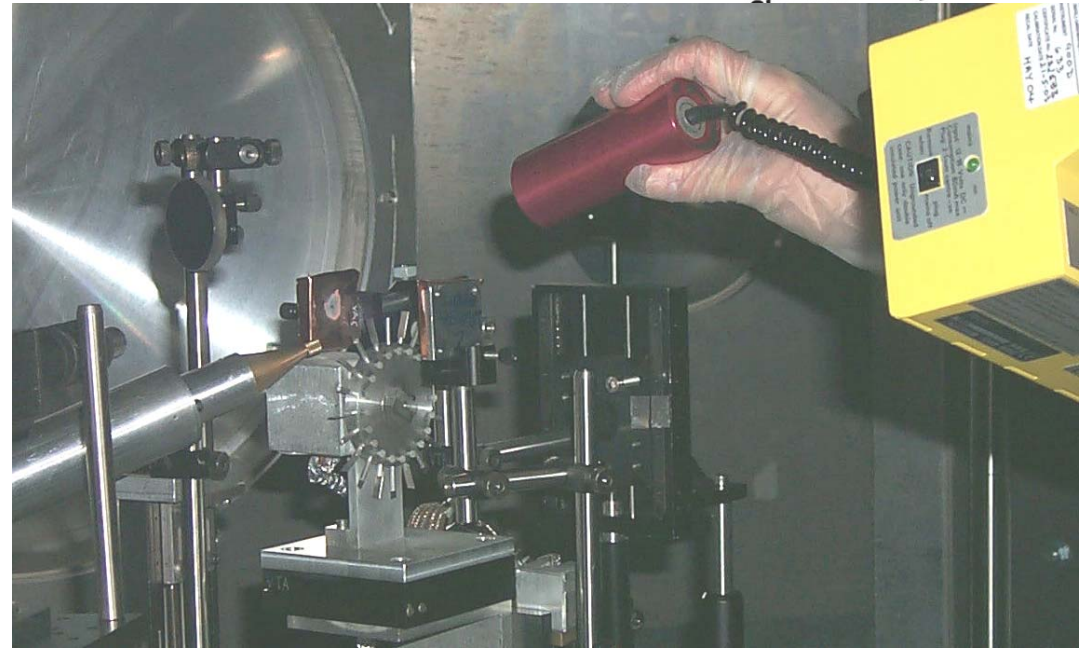
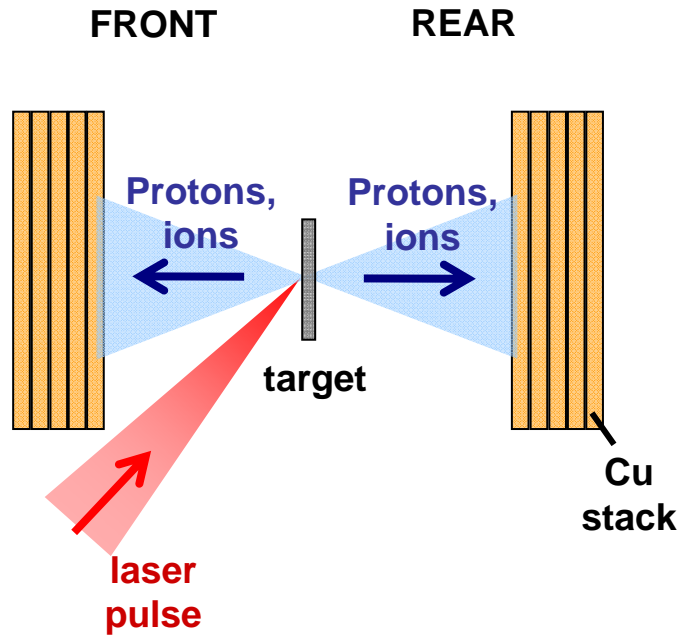
Stacked activation foils: measure at least 1 reaction in each foil



$I(E)$ :  
temperature  
and yield

Uncertainty usually depends on uncertainty in  $\sigma(E)$

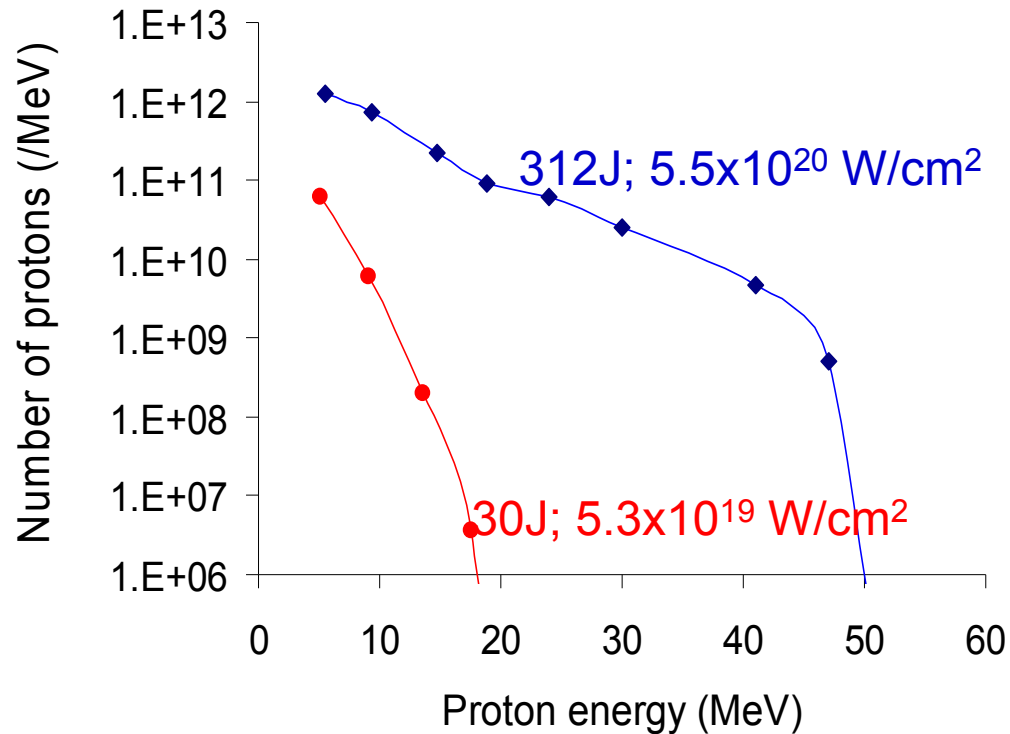
# Proton activation



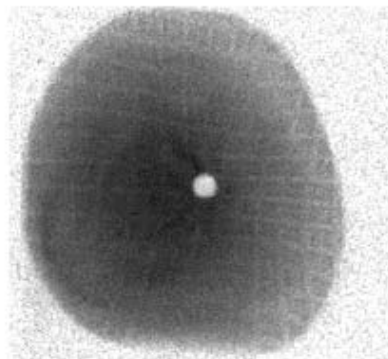
NaI(PMT) detectors  
arranged for  
coincidence  
counting to detect  
positron signature  $\gamma$   
(511 keV)



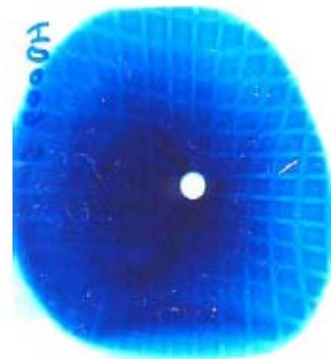
## Example measurements



Cu activation



RCF film



### Advantages:

- 6 orders of magnitude dynamic range
- spatially integrated or resolved proton detection
- Half-life measurement confirms proton activation

### Disadvantages:

- Analysis off-line, time-consuming;
- Relies on knowledge of cross sections
- Limitation on proton upper energy due to other reactions eg Gamma-induced

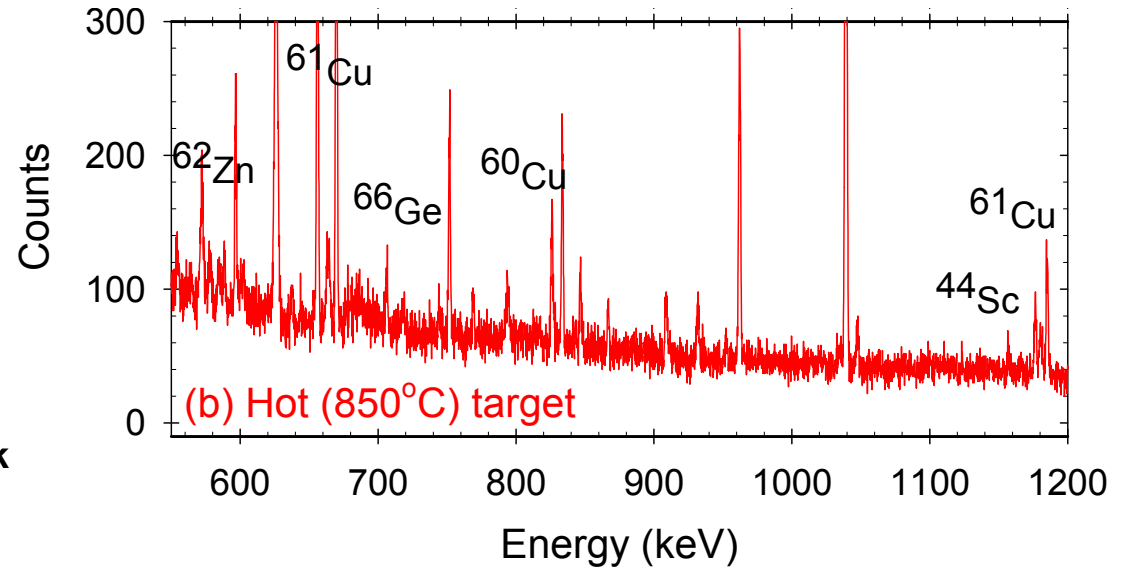
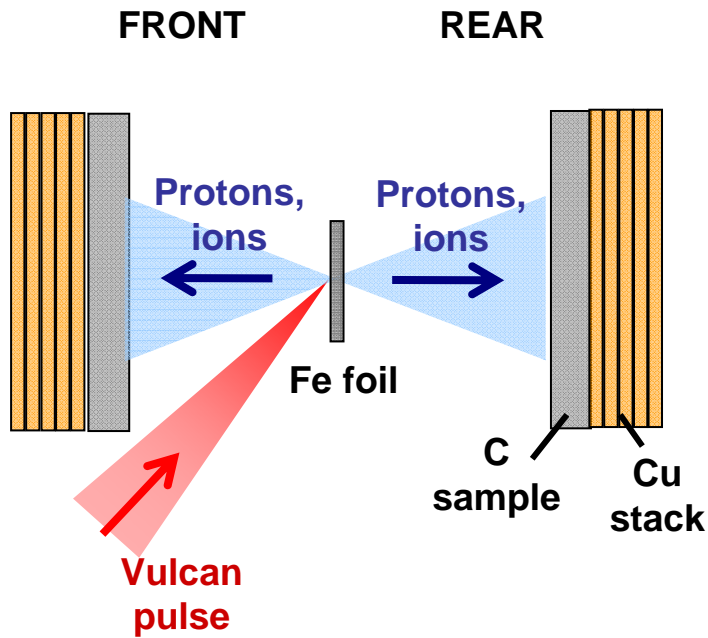


F. Hanachi et al, University of Bordeaux





# Nuclear activation as an ion diagnostic



Cooled high resolution Ge detector



McKenna *et al.*, Phys. Rev. Lett., 91, 075006 (2003)

McKenna *et al.*, Appl. Phys. Lett., 83, 2763 (2003)

McKenna *et al.*, Phys. Rev. E, 70, 036405 (2004)

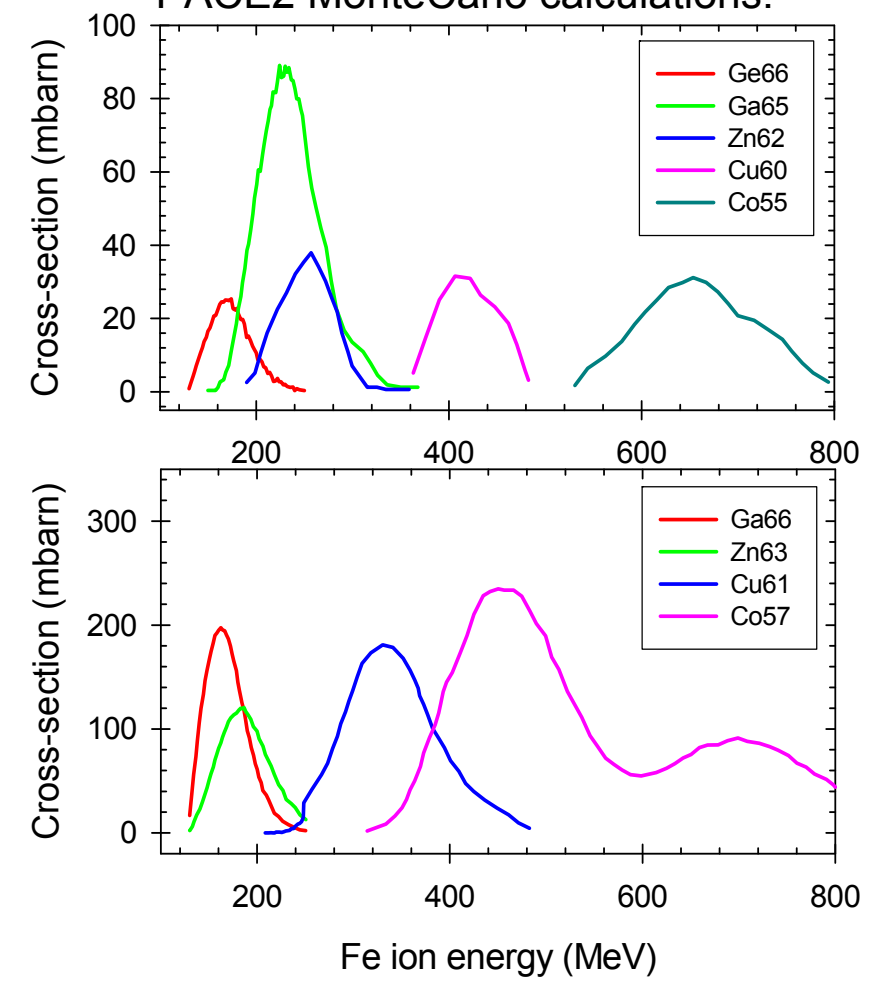


# Ion diagnostic: Fusion-evaporation reactions

				60	61	62	63	64	65	66	67	68	69
			Ge	Ge	Ge	Ge	Ge	Ge	Ge	Ge	Ge	Ge	
			58	59	60	61	62	63	64	65	66	67	
			Ga	Ga	Ga	Ga	Ga	Ga	Ga	Ga	Ga	Ga	
			56	57	58	59	60	61	62	63	64	65	66
			Zn	Zn	Zn	Zn	Zn	Zn	Zn	Zn	Zn	Zn	Zn
			54	55	56	57	58	59	60	61	62	63	64
			Cu	Cu	Cu	Cu	Cu	Cu	Cu	Cu	Cu	Cu	Cu
			52	53	54	55	56	57	58	59	60	61	62
			Ni	Ni	Ni	Ni	Ni	Ni	Ni	Ni	Ni	Ni	Ni
			51	52	53	54	55	56	57	58	59	60	61
			Co	Co	Co	Co	Co	Co	Co	Co	Co	Co	Co
			50	51	52	53	54	55	56	57	58	59	60
			Fe	Fe	Fe	Fe	Fe	Fe	Fe	Fe	Fe	Fe	Fe
			49	50	51	52	53	54	55	56	57	58	59
			Mn	Mn	Mn	Mn	Mn	Mn	Mn	Mn	Mn	Mn	Mn
			48	49	50	51	52	53	54	55	56	57	58
			Cr	Cr	Cr	Cr	Cr	Cr	Cr	Cr	Cr	Cr	Cr
			47	48	49	50	51	52	53	54	55	56	57
			V	V	V	V	V	V	V	V	V	V	V
			46	47	48	49	50	51	52	53	54	55	56
			Ti	Ti	Ti	Ti	Ti	Ti	Ti	Ti	Ti	Ti	Ti
			45	46	47	48	49	50	51	52	53	54	55
			Sc	Sc	Sc	Sc	Sc	Sc	Sc	Sc	Sc	Sc	Sc
			44	45	46	47	48	49	50	51	52	53	54
			Ca	Ca	Ca	Ca	Ca	Ca	Ca	Ca	Ca	Ca	Ca

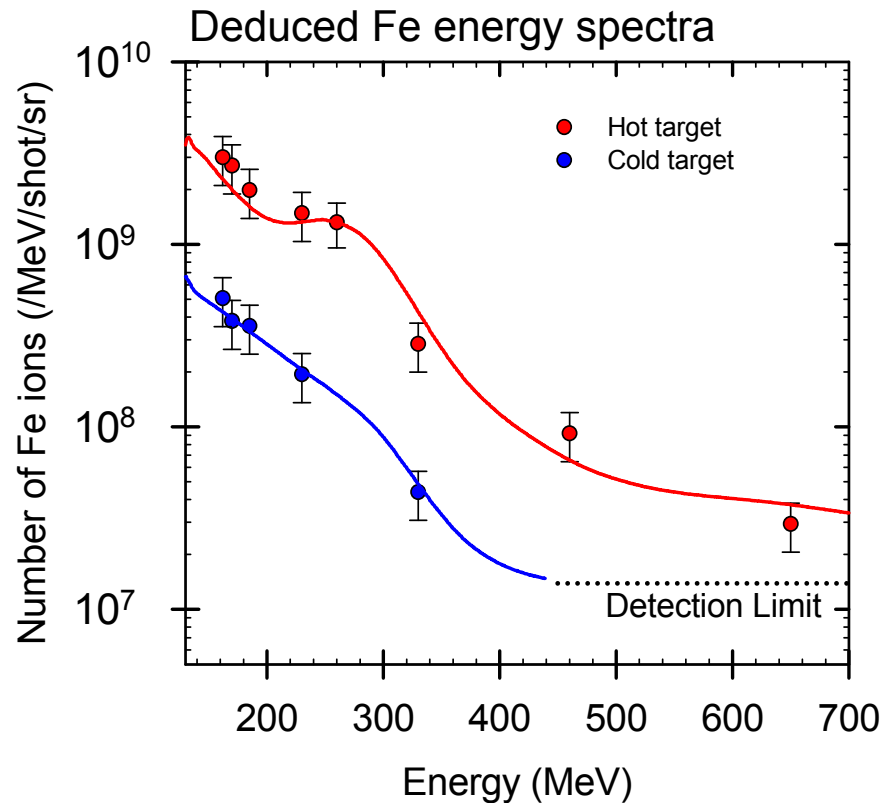
$[^{56}\text{Fe}+^{12}\text{C}]$

PACE2 MonteCarlo calculations:





## Example measurement of ion energy spectra



### Advantages:

- Direct evidence of ion species
- Enables spatially integrated ion detection

### Disadvantages:

- Analysis off-line, time-consuming and cumbersome
- Relies on knowledge of cross sections
- No charge information



University of  
**Strathclyde**  
Glasgow

Thank you for your attention!